JOURNAL OF MATERIALS SCIENCE 22 (1987) 233–238

The relationship between metal fibre morphology and electrical properties of InSb–NiSb eutectic composites

I. S. AHN, I. H. MOON
Department of Materials Engineering, Han Yang University, Seoul, Korea

The dependence of the microstructure on the growth rate and alloying composition in the InSb–NiSb system was investigated in order to determine the formation conditions of the eutectic coupled region of this system and to establish the relationship between the structural anisotropy and the magneto- and electrical resistance in this eutectic-coupled region. The InSb–NiSb alloy of 0.5 to 5 wt% NiSb formed the eutectic-coupled region at a growth rate of 0.5 cm h^{-1}, but the same region was also found in 1 to 3 wt% NiSb alloy grown at the rate of 1 cm h^{-1}. Transverse magnetoresistance seems to be related to the continuity of metal fibre in the case of the eutectic alloy, and it has the highest value at eutectic volume fraction of fibres in the case of alloys whose composition belongs to the eutectic-coupled region.

1. Introduction

Unidirectionally solidified materials have been investigated partly for possible applications of their interesting physical properties, such as the electromagnetic properties of some eutectic systems [1, 2], anisotropic electrical resistivity [3, 4], the aligned p–n heterogeneous junctions of eutectics [5] and multineedle cathode of Ni–W eutectic composite [6]. Such physical properties of the unidirectionally solidified eutectic alloys are strongly dependent on the microstructural anisotropy as well as the physical properties of an individual constituent element of the pertinent alloy system. After the classification by Weiss [7] the eutectic composites that combined the semiconductor matrix with the metal inclusion would be expected to show the composite effect in galvanomagnetic, thermal and optical properties. Therefore, many investigations have been carried out on the system consisting of the aligned metal inclusion in the matrix of the III–V group compound semiconductors [7–10]. The eutectic system of the InSb compound semiconductor matrix and metal inclusion belongs to one of the commonly investigated systems, because it has the highest electron mobility (76 000 $cm^2 V^{-1} sec^{-1}$) among the compound semiconductors.

The InSb–NiSb eutectic system has some interesting properties; it has a highly aligned metal fibre of the order of 1 μm diameter and a eutectic composition of a relatively low volume fraction of NiSb phase. Therefore elucidation of the relationship between the microstructure and the electrical properties of the InSb–NiSb system is one important subject for the possible application of the composite system.

Up to now a number of eutectic systems have been proved to exhibit the anisotropy of their physical properties owing to alignment of the second-phase inclusion [11]. This suggests strongly that the microstructural parameter might uniquely correlate with the measured physical property. Several investigations have been carried out on the electrical resistivity in the aligned eutectic morphology [9, 12–14]. In particular, such a eutectic morphology was characterized by continuity of fibres in the growth direction from electrical resistivity measurement [13].

Since the InSb–NiSb eutectic system has high magnetoresistance properties due to the highly aligned metal fibre, the relationship between electrical properties and volume fraction of metal fibre should be clarified in the eutectic-coupled region, where the aligned metal fibre exists in the semiconductor matrix. The aim of the present work is to investigate the dependence of the microstructure on the growth rate and alloying composition in the InSb–NiSb system in order to determine the formation conditions of the eutectic-coupled region of this system and to establish the relationship between the structural anisotropy and the magneto- and electrical resistance.

2. Experimental techniques

The alloys were made from indium with a minimum purity of 99.999%, nickel of 99.99% and antimony of 99.99%. InSb–NiSb alloys containing 0.5 to 5 wt% NiSb were prepared by melting a stoichiometric amount of the raw metals under a vacuum pressure of 5×10^{-4} torr in a sealed silica tube. Prior to unidirectional solidification, the alloy specimens were held for 4 h in the melting zone of the furnace for homogenization.

The temperature gradient of 200° C cm^{-1} was maintained by circulating the cooling water below the heating zone. Growth rates were varied from 0.5 to 5 cm h^{-1}.

After solidification, each end, 5 mm away from the top and the bottom of the unidirectionally grown crystals, was discarded for the purpose of removing the initial and final transient regions. The remaining

0022–2461/87 $03.00 + .12

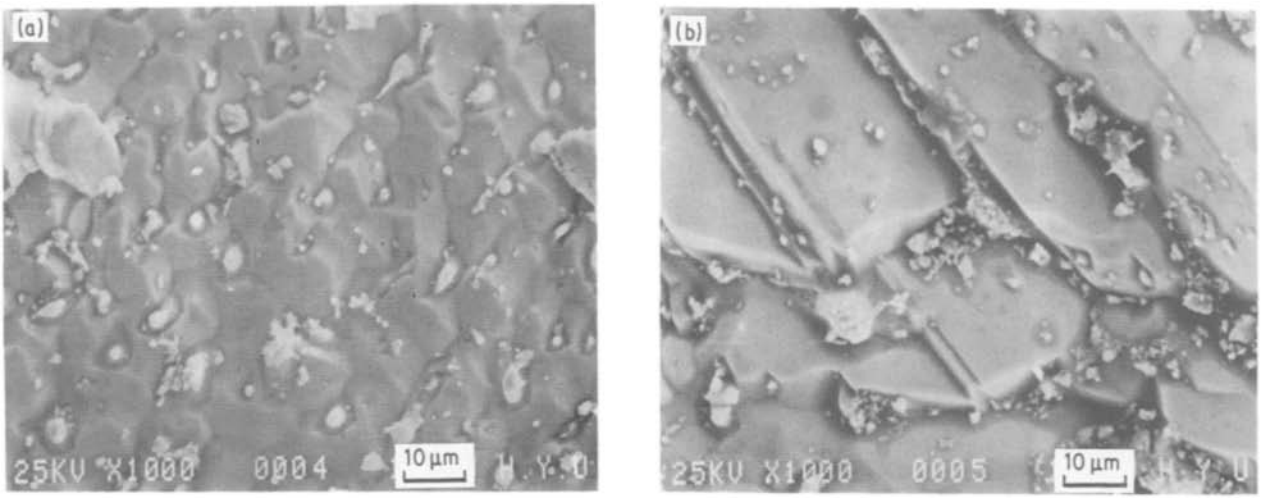

Figure 1 Scanning electron microscopy (SEM) picture of solid/liquid interface morphology of InSb–5 wt % NiSb alloy grown at 6 cm h^{-1} (a) Flat interface, (b) inclined interface.

length of the specimen was 30 mm. The crystals were cut into a transverse and longitudinal section with a microdiamond cutter in order to prepare the metallographic specimens.

The continuity of the metal fibre was measured in the microstructural photographs at a magnification of × 300 and × 1000 by measuring the length of an NiSb fibre in the growth direction. Specimens for the measurement of electrical properties were prepared by cutting the crystal section parallel to the transverse and longitudinal directions. The size of the specimen cut parallel to the transverse direction was 1.2 to 1.3 mm × 0.5 to 0.6 mm cross-section and 6 to 7 mm long, but the specimens prepared parallel to the longitudinal direction were 13 to 15 mm long, with the same cross-section.

The electrical resistivity of the prepared specimens was measured with a Wheatstone Bridge at room temperature (with maximum error limits of ±9%). Both ends of a specimen were soldered by indium in order to ensure good ohmic contact. The transverse magnetoresistance was also measured in a magnetic field of 6000 G at room temperature.

3. Results and discussion

3.1. Microstructure

Fig. 1 shows the microphotographs of the sold/liquid interface obtained by the decanting method, which rapidly removes the remaining liquid by means of upsetting the silica tube after taking it out of the furnace during solidification. Fig. 1a shows the flat surface of the solid/liquid interface in the central area of the InSb–5 wt % NiSb alloy crystal grown at a rate of 6 cm h^{-1}, while the inclined surface near the tube wall was due to the transverse temperature gradient as shown in Fig. 1b.

The InSb–NiSb alloy system showed a typical faceted/nonfaceted (f–nf) growth morphology. The metal fibre was set in the faceted InSb semiconductor matrix. It is also well known that the eutectic system with the low volume fraction of the second-phase usually forms a fibrous or rod-like structure at any growth rate [15].

Fig. 2 shows the dependence of longitudinal microstructure of the InSb–NiSb alloy system on alloy composition as well as growth rate. As shown in this figure, neither a primary InSb crystal nor a primary NiSb crystal was observed for alloys of exact eutectic composition at all growth rates investigated in this work. However, the metal fibre has an inhomogeneous distribution in the InSb matrix in the case of the higher growth rate. Primary InSb and primary NiSb crystals were formed at the higher growth rates both in the alloy of hypocomposition and of hypercomposition.

It is generally believed that the coupled region of the f-nf alloy is skewed toward the faceted composition [16, 17]. However, a typical skewed coupled region could not be observed in the present system in the region of the growth rate investigated here.

Burden and Hunt [18] suggested, with the aid of a competitive model, that the coupled region could be specified by the following relation;

$$\Delta c = A(GD/R) + B(R^{1/2}) \quad (1)$$

where A and B are constant, G is a temperature gradient, R is the growth rate, D is the diffusion coefficient and Δc is the composition range within which a fully eutectic structure can be obtained. The aligned eutectic structure of the non-eutectic composition alloy obtained by solidifying at a lower growth might be explained by the above relationship. Fig. 3 shows the transverse and longitudinal microstructures obtained at growth rates of 0.5 and 1 cm h^{-1} in the eutectic composition.

3.2. Electrical properties of the eutectic

Fig. 4 shows the dependence of the measured electrical resistivity on the growth rate in the eutectic composition. The largest difference of the electrical resistivity between a transverse and a longitudinal direction (about 1.51 × 10^{-4} Ω cm) was observed for the eutectic alloy grown at a growth rate of 0.5 cm h^{-1}.

The resistivity difference between two perpendicular directions was decreased with increase in growth rate. Such an electrical anisotropy should be attributed to the structure anisotropy due to alignment of the metal fibre in the InSb semiconductor matrix. Structural

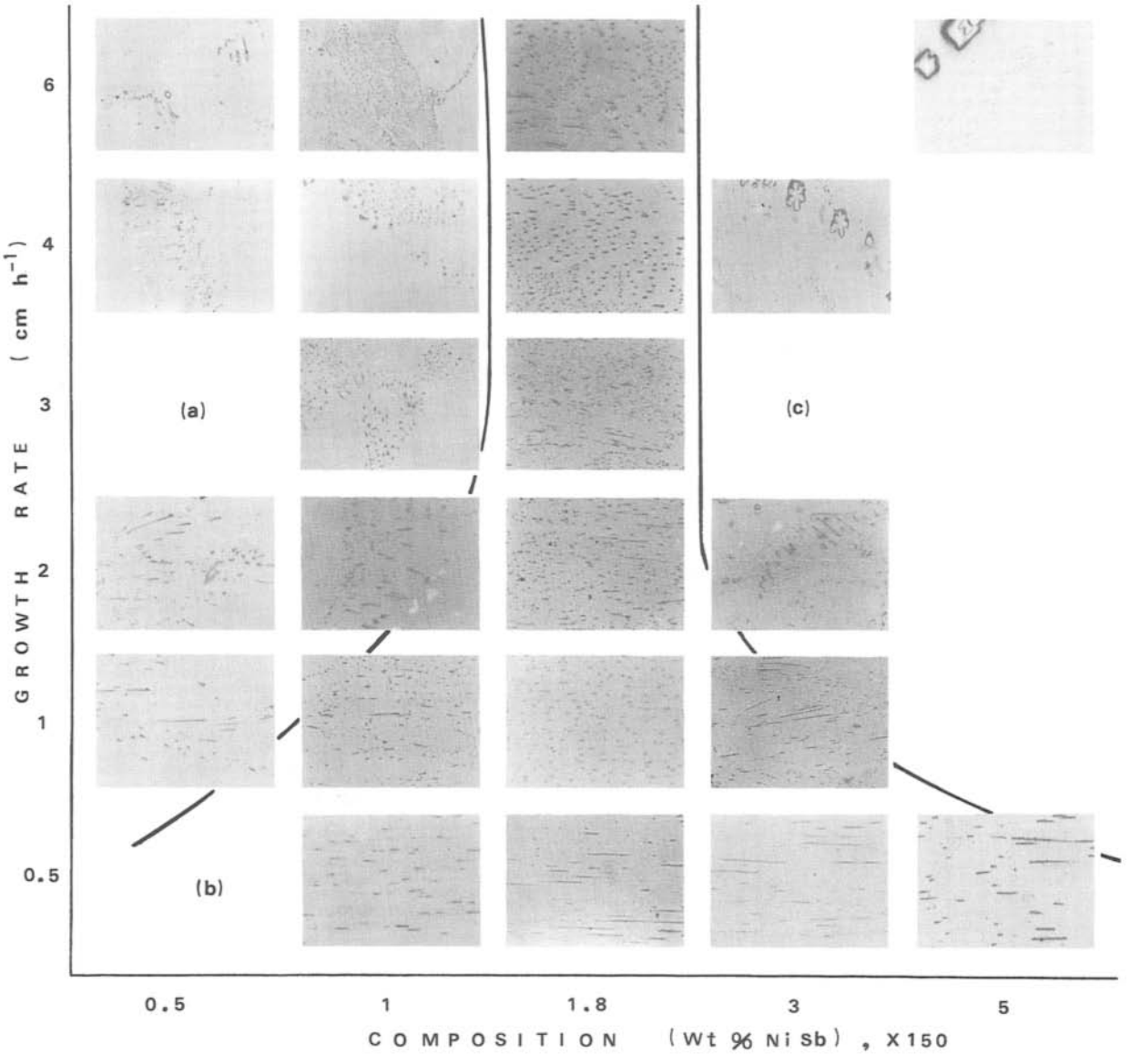

Figure 2 Microstructure of InSb–NiSb eutectic system as a function of alloy composition and growth rate. (a) Primary InSb, (b) eutectic couple, (c) primary NiSb.

anisotropy could be explained with a conception of continuity.

Since NiSb fibres are finite in length parallel to the growth direction, the per cent continuity (X) may be defined as

$$X = 100 \sum_i \frac{L - Z_i}{L} \tag{2}$$

where Σ_i represents the summation along a given reference plane parallel to and passing through the fibres in the growth direction. Z_i is the minimal separation in the growth direction between fibres in the given reference plane and L is the length of the specimen examined.

From the electrical circuit based on the microstructure suggested by Digges and Tauber [13], the electrical resistivity parallel and perpendicular to the growth direction can be described as;

$$\varrho_{\parallel} = \frac{1 - (V_{\mathrm{NiSb}}/X)}{\varrho_{\mathrm{InSb}_{\parallel}}} + \frac{V_{\mathrm{NiSb}}}{X[\varrho_{\mathrm{NiSb}} X + \varrho_{\mathrm{InSb}_{\parallel}}(1 - X)]} \tag{3}$$

$$\varrho_{\perp} = \frac{1 - X}{\varrho_{\mathrm{InSb}_{\perp}}} + \frac{X^2}{\varrho_{\mathrm{InSb}_{\perp}}(X - V_{\mathrm{NiSb}}) + \varrho_{\mathrm{NiSb}} V_{\mathrm{NiSb}}} \tag{4}$$

where $\varrho_{\parallel}$ is the resistivity of eutectic alloy parallel to the growth direction, $\varrho_{\perp}$ is the resistivity of eutectic alloy perpendicular to the growth direction, X is the continuity (as value of fraction) of the consolidated fibres, $\varrho_{\mathrm{InSb}_{\parallel}}$ is the resistivity of InSb parallel to the growth direction, ϱ_{NiSb} is the resistivity of NiSb and V_{NiSb} is the volume fraction of NiSb. $\varrho_{\mathrm{InSb}_{\perp}}$ is the resistivity of InSb normal to the growth direction.

In the present experiment, the continuity (X) decreased exponentially with increasing growth rate as shown in Fig. 5, and this relation can be expressed in the following form

$$X = a \exp(-bR) + c \tag{5}$$

where X is continuity of the NiSb fibre and R is the growth rate (cm h^{-1}). In the present system, $a = 0.34$, $b = 0.22$ and $c = 0.024$ were obtained as constants. As anisotropy of the impurity-doped InSb crystal is also related to growth rate, the electrical resistivity was measured for all InSb crystal which were prepared

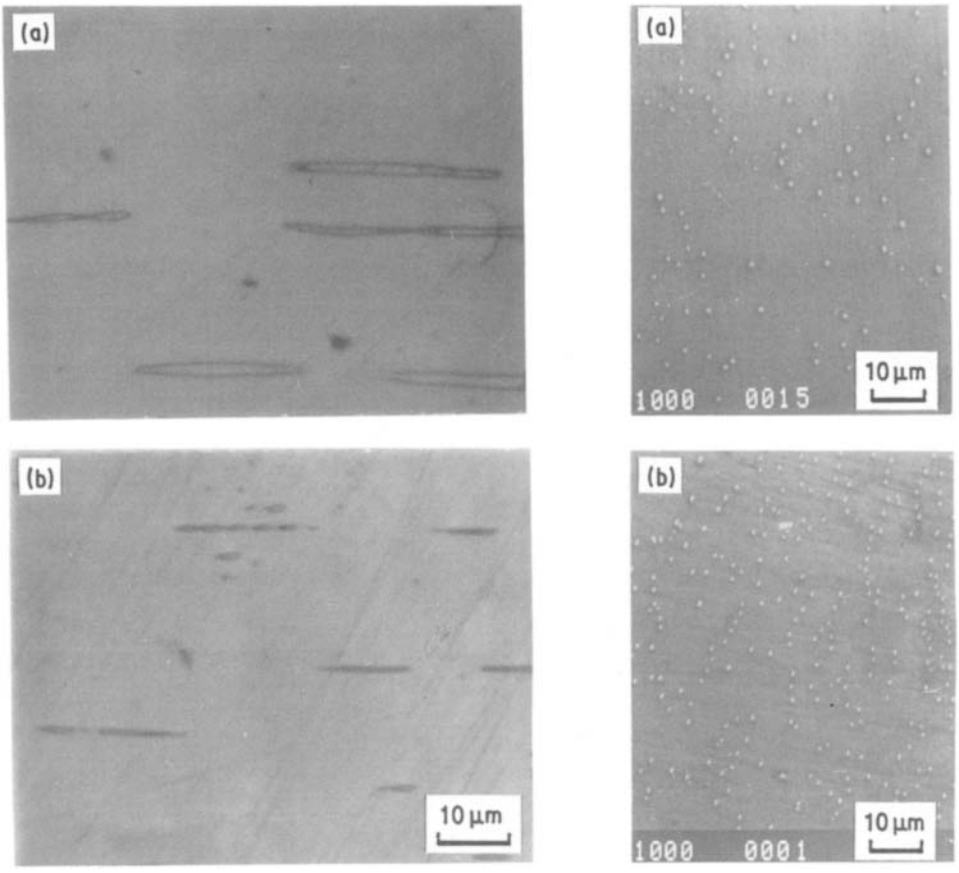

Figure 3 Microstructure of eutectic alloy. (a) Grown at 0.5 cm h^{-1}, (b) grown at 1 cm h^{-1}, (right) transverse (left) longitudinal.

by solidifying at various growth rates. By putting the measured electrical resistivity of InSb crystal and the resistivity data of nickel and antimony found in the literature [19] into Equations 3 and 4, the electrical resistivity of the InSb–NiSb alloy system was calculated as a function of growth rate.

Fig. 6 shows that the experimental values agreed relatively well with the calculated ones. The measured magnetoresistance in the transverse direction was somewhat higher than that in the longitudinal direction as shown in Fig. 7. The magnetoresistance of the systems also decreased with increasing growth rate. This behaviour indicates that there should be some relationship between the magnetoresistance and continuity of fibres, as partly discussed in following section.

3.3. Electrical properties of the coupled region

The electrical resistivity was also measured for alloys of hypo- and hypereutectic composition. Figs 8 and 9 show the resistivity difference between two perpendicular directions for the specimens of InSb–1 wt % and InSb–2 wt % NiSb, respectively. The resistivity difference increased with decrease in growth rate. This behaviour also agreed with the microstructural anisotropy, because volume fraction of the primary phase increased with the increase in growth rate higher than 2 cm h^{-1} as shown in Fig. 2.

An aligned eutectic structure was also obtained at low growth rate in specimens whose composition ranged from 0.5 to 5 wt % NiSb. The dependence of the magnetoresistivity and electrical resistivity on the

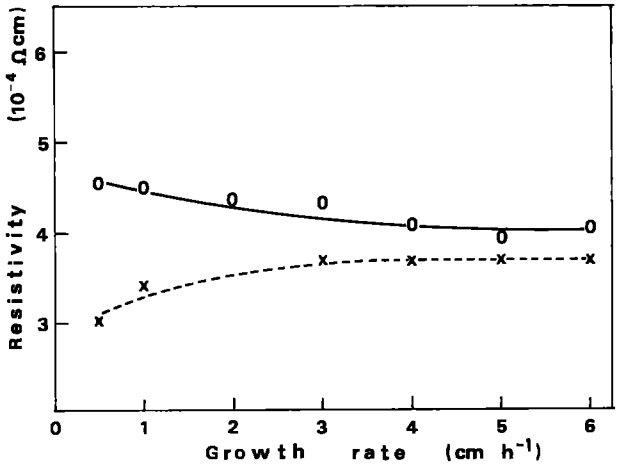

Figure 4 Resistivity of eutectic alloy at various growth rates. (○) Transverse, (×) longitudinal directions.

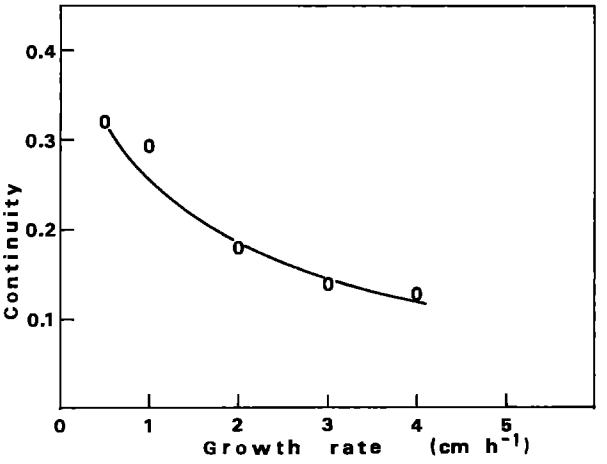

Figure 5 Relationship between continuity and growth rate of eutectic alloy.

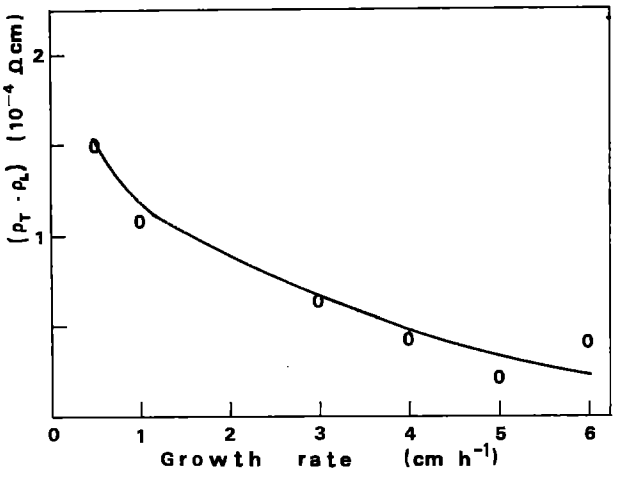

Figure 6 Resistivity difference of eutectic alloy at various growth rates (O) Measured values, (——) calculated values.

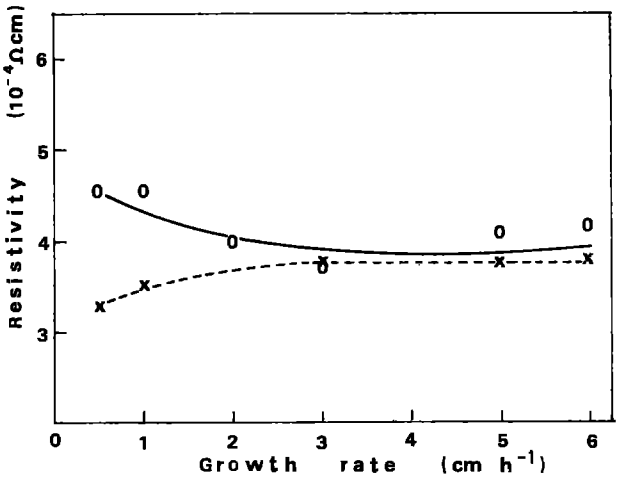

Figure 8 Resistivity of hypoeutectic (1 wt % NiSb) alloy at various growth rates. (O) Transverse direction, (×) longitudinal direction.

fibre fraction could be examined for specimens grown at a rate of 1 or 0.5 cm h^{-1}. The electrical resistivity of the above specimens decreased with increase in volume fraction of NiSb metal fibres as shown in Fig. 10. It can be determined from the continuity of NiSb fibres.

In the InSb–NiSb system, the continuity of the fibre was found to increase slightly with increase in the volume fraction of a fibre phase as shown in Fig. 11. The slight decrease of electrical resistivity on increasing the volume of NiSb fibre as shown in Fig. 10, might be related to such an increase of the fibres continuity due to increase of its volume fraction. However, the highest magnetoresistance could be obtained at the eutectic composition, because the highest structural anisotropy, which is related to the resistivity difference, was observed at the eutectic composition as shown in Fig. 12.

The dependence of magnetoresistance on the volume fraction of NiSb cannot be explained on the concept of continuity only, because continuity is related to structural anisotropy as well as composition. Therefore, the relationship between magnetoresistance and volume fraction of NiSb should be determined for the alloys which have the same structural anisotropy. The same degree of anisotropy was obtained for three specimens, which had an NiSb composition of 5, 1.8 and 1 wt % and were grown at 0.5, 1 and 1 cm h^{-1}, respectively, as shown in Fig. 12. Among the three specimens the highest magnetoresistance was obtained in the specimen of 1.8 wt % NiSb grown at 1 cm h^{-1}.

4. Conclusions

1. The continuity of the fibre phase NiSb in InSb–NiSb alloy was decreased exponentially by increasing the growth rate.

2. The relationship between electrical resistivity and growth rate was proved by measuring the continuity of the NiSb fibre.

3. The aligned eutectic structure was obtained at a growth rate of 0.5 cm h^{-1} in the InSb–NiSb alloy with NiSb composition of 0.5 to 5 wt %, but the same structure was obtained at a growth rate of 1 cm h^{-1} in the alloy of 1 to 3 wt % NiSb.

4. The highest structural anisotropy was found in the eutectic composition and at a growth rate of 0.5 or 1 cm h^{-1}.

5. Transverse magnetoresistance seems to be related to the continuity of metal fibre in the case of the eutectic alloy, and it has the highest value at the eutectic volume fraction of fibres.

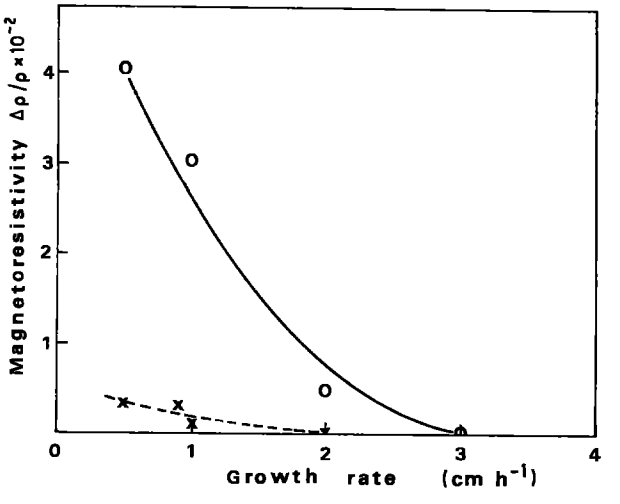

Figure 7 Magnetoresistivity of eutectic alloy at various growth rates. (O) Transverse direction, (×) longitudinal direction.

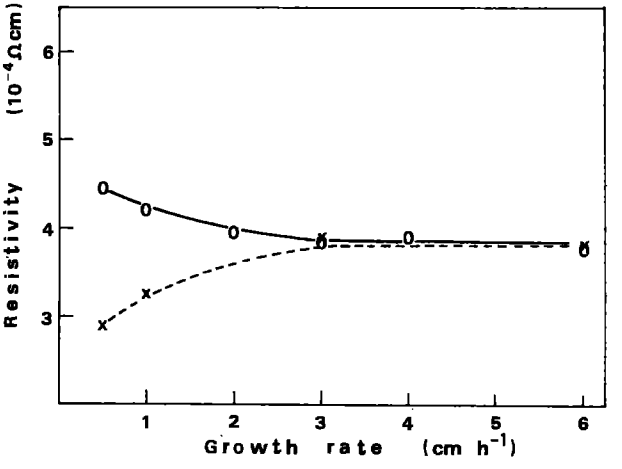

Figure 9 Resistivity of hypereutectic (3 wt % NiSb) alloy at various growth rates. (O) Transverse direction, (×) longitudinal direction.

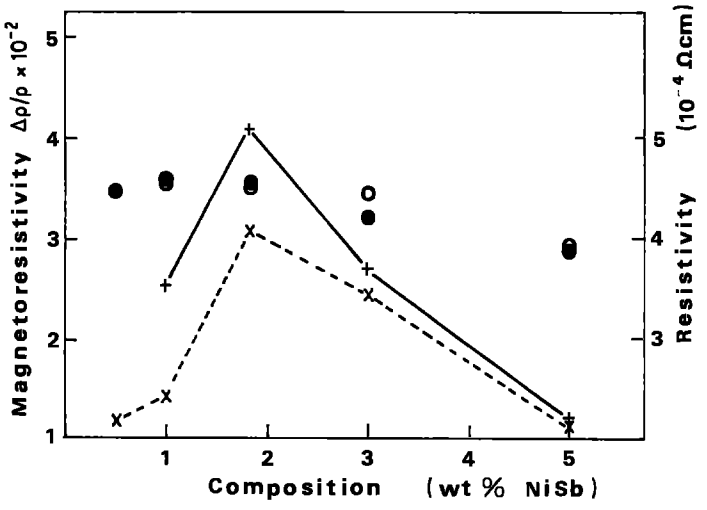

Figure 10 Magnetoresistivity and resistivity at various compositions of a euetectic alloy in the transverse direction. (o) 0.5 cm h^{-1} resistivity, (●) 1 cm h^{-1} resistivity, (+) 0.5 cm h^{-1} $\Delta\varrho/\varrho$, (×) 1 cm h^{-1} $\Delta\varrho/\varrho$.

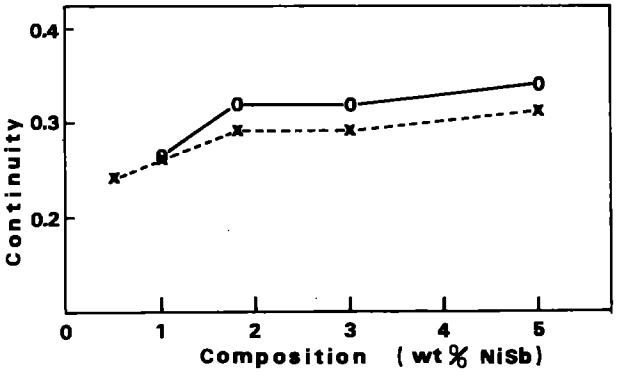

Figure 11 Relationship between continuity and composition in the eutectic coupled region. (o) 0.5 cm h^{-1}, (×) 1 cm h^{-1}.

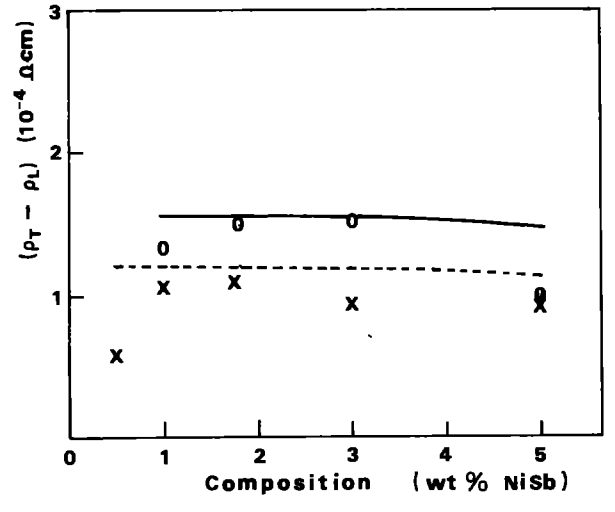

Figure 12 Relationship between resistivity difference and composition in the eutectic coupled region. (o) 0.5 cm h^{-1} measured, (×) 1 cm h^{-1} measured, (——) 0.5 cm^{-1} calculated, (– – –) 1 cm h^{-1} calculated.

Acknowledgement

The authors would like to thank KOSEF for the research scholarship to one of the authors (I.S.A.).

References

1. H. WEISS and M. WILHELM, *Z. Physik.* **176** (1963) 399.
2. M. R. JACKSON, R. N. TAUBER and R. W. KRAFT, *J. Appl. Phys.* **39** (1968) 4452.
3. LIONEL M. LEVINSON, *Appl. Phys. Lett.* **21** (1972) 289.
4. I. H. MOON, Y. L. KIM and I. S. AHN, *J. Mater. Sci.* **16** (1981) 1367.
5. W. ALBERS and J. VERBERKT, *ibid.* **5** (1970) 24.
6. H. E. CLINE, *J. Appl. Phys.* **41** (1970) 76.
7. H. WEISS, *Met. Trans.* **2** (1971) 1513.
8. F. S. GALASSO, *J. Metals.* **19** (1967) 17.
9. W. M. KIM and E. J. STOPKO, *J. Appl. Phys.* **38** (1967) 5211.
10. B. PAUL, H. WEISS and M. WILHELM, *Solid State Electronics* **7** (1964) 835.
11. F. S. GALASSO, F. C. DOUGLAS and J. A. BATT, *J. Metals* **22** (1970) 40.
12. W. K. LIEBMANN and E. A. MILLER, *J. Appl. Phys.* **34** (1963) 2653.
13. T. G. DIGGES, Jr and R. N. TAUBER, *Met. Trans.* **2** (1971) 1683.
14. W. G. WATSON, W. C. HAHN, Jr. and R. W. KRAFT, *ibid.* **6A** (1975) 151.
15. M. N. CROKER, D. BARAGAR and R. W. SMITH, *J. Crystal Growth* **30** (1975) 198.
16. D. J. FISHER and W. KURZ, in "Proceedings of International Conference on Solidification and Casting", Sheffield, July 1977, edited by B. B. Argent (The Metals Society, London, 1979) p. 57.
17. G. A. CHADWICK, "Metallography of phase transformations" (Butterworths, London, 1972) p. 126.
18. M. H. BURDEN and J. D. HUNT, *J. Crystal Growth* **22** (1974) 328.
19. C. J. SMITHELLS, "Metals Reference Book" (Butterworth, London, Boston, 1976) p. 1035.

Received 21 January
and accepted 6 May 1986